Organometallic Chalcogen Complexes. XXII. Syntheses and Structural Analyses by X-Ray Diffraction and Electron Spin Resonance Single-Crystal Methods of $Co_3(CO)_9Se$, $FeCo_2(CO)_9Se$, and $FeCo_2(CO)_9Te$. The Antibonding Metallic Nature of an Unpaired Electron in an Organometallic Cluster System[1,2]

Charles E. Strouse[3] and Lawrence F. Dahl*

Contribution from the Department of Chemistry, University of Wisconsin, Madison, Wisconsin 53706. *Received February 22, 1971*

Abstract: The preparation of the three metal cluster compounds $Co_3(CO)_9Se$, $FeCo_2(CO)_9Se$, and $FeCo_2(CO)_9Te$ by different reactions and their subsequent characterization by X-ray diffraction and esr single-crystal methods were carried out in order to provide operational proof for the previously demonstrated antiaromatic character of the unpaired electron in the tricobalt fragment contained in the $Co_3(CO)_9S$ molecule (of C_{3v} geometry), as well as to determine the effect of this least stable valence electron on the molecular parameters of such a triangular metal cluster system upon change of the triply bridging chalcogen ligand. In addition to giving important stereochemical information concerning the first quantitative characterization of the distribution of valence electrons in an organometallic cluster system, this investigation has general significance in clearly demonstrating that any electrons in excess of the closed-shell electronic configuration of each metal atom in a triangular metal cluster system will occupy primarily the *antibonding* metal σ orbitals (in an equivalent orbital formalism) and thereby will reduce the *net* metal–metal valence bond order to a value *less* than *one*. As in the case of $Co_3(CO)_9S$, the esr studies of $Co_3(CO)_9Se$ in solution and doped in single crystals of $FeCo_2(CO)_9Se$ have shown that the unpaired electron in $Co_3(CO)_9Se$ resides in an MO (of a_2 representation) which is made up primarily of an antibonding combination of cobalt 3d orbitals localized in the plane of the three cobalt atoms. The close similarity of the hyperfine parameters of $Co_3(CO)_9Se$ with those of $Co_3(CO)_9S$ substantiates the prediction that the chalcogen atom has little effect on the half-filled a_2 orbital. These results and the detailed changes in metal–metal distances in the series $FeCo_2(CO)_9X$ (X = S, Se, Te) and $Co_3(CO)_9X$(X = S, Se) are interpreted in light of the structure and bonding of these organometallic clusters. Direct bond-length evidence of the antibonding metallic character of the unpaired electron in $Co_3(CO)_9Se$ is shown from the fact that its removal by formal replacement of one cobalt atom with an iron atom to give $FeCo_2(CO)_9Se$ gives rise to an average *decrease* of 0.039 (1) Å in the chemically equivalent metal–metal bond lengths (based on an assumed crystal-disordered model in the case of $FeCo_2(CO)_9Se$). The markedly *decreased* antibonding effect of the unpaired electron on the metal–metal distances in the two selenium complexes, in contrast to the more dramatic effect on the metal–metal distances in the two corresponding sulfur analogs, is also reflected by an average *decrease* of 0.021 (4) Å in the cobalt–cobalt distances upon substitution of the larger congener selenium for a sulfur atom in $Co_3(CO)_9S$. The structural determinations of $Co_3(CO)_9Se$, $FeCo_2(CO)_9Se$, and $FeCo_2(CO)_9Te$ (of different crystal structure from $Co_3(CO)_9S$ and the isomorphous $FeCo_2(CO)_9S$) show each of the three compounds to crystallize with four molecules in a centrosymmetric triclinic unit cell of symmetry $C\bar{1}$. The lattice parameters (with estimated precisions given in parentheses) are $a = 9.503(1)$, $b = 13.918(1)$, $c = 14.123(1)$ Å, $\alpha = 114.32$, $\beta = 117.75$, $\gamma = 84.56°$ for $Co_3(CO)_9Se$; $a = 9.460(1)$, $b = 13.842(1)$, $c = 14.091(1)$ Å, $\alpha = 114.01$, $\beta = 117.66$, $\gamma = 84.61°$ for $FeCo_2(CO)_9Se$; and $a = 8.773$ (16), $b = 15.205$ (29), $c = 14.578$ (28) Å, $\alpha = 117.29$, $\beta = 118.73$, $\gamma = 78.42°$ for $FeCo_2(CO)_9Te$. The crystal packing of $FeCo_2(CO)_9Se$ is virtually identical with that of $Co_3(CO)_9Se$ but significantly different from that of $FeCo_2(CO)_9Te$. The particular interrelationship between the crystal packing of the two selenium compounds and that of the $Co_3(CO)_9S$ and $FeCo_2(CO)_9S$ compounds was correctly deduced from the single-crystal esr and preliminary X-ray measurements. The structural determinations were performed with a Datex-controlled General Electric diffractometer; anisotropic least-squares refinements (which initially utilized a procedure involving the noncrystallographic constraining of the one independent molecule per unit cell to exact C_{3v} symmetry) yielded unweighted discrepancy factors of $R_1 = 0.043$ for $Co_3(CO)_9Se$, 0.030 for $FeCo_2(CO)_9Se$, and 0.023 for $FeCo_2(CO)_9Te$.

X-Ray structural determinations of the paramagnetic $Co_3(CO)_9S$[4] and of the isomorphous diamagnetic mixed-metal analog $FeCo_2(CO)_9S$[1] first indicated the nature of the partially filled molecular orbital of $Co_3(CO)_9S$ in that they furnished direct bond-length evidence that this orbital containing the unpaired electron is composed primarily of an *antibonding* combination of cobalt atomic orbitals. The paramagnetism of $Co_3(CO)_9S$ along with the existence of the isomorphous diamagnetic $FeCo_2(CO)_9S$ as a host material provided a unique opportunity to employ dilute single-crystal esr techniques to elucidate the quantitative distribution of an unpaired electron in an organometallic cluster system. In agreement with the X-ray results, an esr investigation[5] of $Co_3(CO)_9S$ doped in the $FeCo_2(CO)_9S$ disclosed that the unpaired electron in the $Co_3(CO)_9S$ molecule of idealized C_{3v}-3*m* geometry resides in a non-

(1) Previous paper in this series: D. L. Stevenson, C. H. Wei, and L. F. Dahl, *J. Amer. Chem. Soc.*, **93**, 6027 (1971).

(2) Presented in part at the 157th National Meeting of the American Chemical Society, Minneapolis, Minn., April 1969.

(3) This paper is based in part on a dissertation submitted by C. E. Strouse to the Graduate School of the University of Wisconsin in partial fulfillment of the requirements for the Ph.D. degree, June 1969.

(4) C. H. Wei and L. F. Dahl, *Inorg. Chem.*, **6**, 1229 (1967).

(5) C. E. Strouse and L. F. Dahl, *Discuss. Faraday Soc.*, No. 47, 93 (1969).

degenerate orbital (of a_2 character) which consists mainly of an antibonding combination of cobalt d orbitals localized in the plane of the three cobalt atoms. Since an a_2 molecular orbital is orthogonal to any atomic orbitals on the sulfur atom, it was predicted[5] that there would be little change in the hyperfine parameters of the esr spectrum upon substitution of the congener selenium for sulfur.

To test this hypothesis and to determine on a more general basis the extent that the molecular geometry of other similar complexes would be influenced by a corresponding unpaired electron, the synthesis and characterization by single-crystal X-ray and esr methods of the selenium and tellurium analogs of $Co_3(CO)_9S$ and $FeCo_2(CO)_9S$ were undertaken. The resulting work presented here has yielded further definitive stereochemical information of prime importance with regard to providing a basic understanding of the nature of metal–metal interactions in organometallic cluster systems.

Experimental Section

Preparation of the Complexes. Although $Co_3(CO)_9S$ has been prepared by the reaction of $Co_2(CO)_8$ with a variety of sulfur-containing organic compounds as well as elemental sulfur,[6,7] the attempted reactions of $Co_2(CO)_8$ with elemental selenium, cobalt selenide, and diphenylselenium resulted in the recovery of only the starting materials. Success was finally achieved by the reaction of $Co_2(CO)_8$ in hexane solution with a stoichiometric amount of H_2Se for two days at 150° under 100 atm of carbon monoxide. This reaction produced a good yield of $Co_3(CO)_9Se$ in the form of large brown crystals which are soluble in most organic solvents. Like its sulfur analog, $Co_3(CO)_9Se$ is unstable to air oxidation, especially in solution.

The mixed-metal complex $FeCo_2(CO)_9Se$ was prepared by the reaction of stoichiometric amounts of $Co_2(CO)_8$, $Fe_3(CO)_{12}$, and H_2Se at 150° under 100 atm of carbon monoxide. In order to free the product from small amounts of paramagnetic impurities crystals of $FeCo_2(CO)_9Se$ were dissolved in hexane, and oxygen was allowed to bubble through the solution. The solution was then filtered and the $FeCo_2(CO)_9Se$ was recrystallized. Elemental analysis[8] of this purified material gave the following results. *Anal.* Calcd for $FeCo_2(CO)_9Se$: C, 21.4; O, 28.5; Se, 15.6; Fe, 11.1; Co (by difference), 23.4. Found: C, 21.2; O, 28.3; Se, 15.8; Fe, 10.9; Co (by difference), 23.8. The infrared spectra of $Co_3(CO)_9Se$ and $FeCo_2(CO)_9Se$ are nearly identical with those of the corresponding sulfur analog.[6,7,9]

Although attempts to prepare $Co_3(CO)_9Te$ were unsuccessful, the reaction of stoichiometric amounts of $Co_2(CO)_8$ and $Fe_3(CO)_{12}$ with $(C_2H_5)_2Te$ produced a 30% yield of $FeCo_2(CO)_9Te$. This compound, like the sulfur and selenium analogs, is brown in color, readily soluble in most organic solvents, and very stable in air at room temperature. Its infrared spectrum is nearly identical with those of the sulfur and selenium analogs. *Anal.*[8] Calcd: Fe, 10.1; Te, 23.1; C, 19.5; O, 26.0; Co (by difference), 21.3. Found: Fe, 10.0; Te, 23.2; C, 19.6; O, 25.8; Co (by difference), 21.2.

(6) (a) L. Markó, G. Bor, and E. Klumpp, *Chem. Ind. (London)*, 1491 (1961); (b) L. Markó, G. Bor, E. Klumpp, B. Markó, and G. Alma'sy, *Chem. Ber.*, **96**, 955 (1963); (c) S. A. Khattab, L. Marko, G. Bor, and B. Markó, *J. Organometal. Chem.*, 1, 373 (1964).

(7) C. E. Strouse, unpublished work.

(8) Alfred Bernhardt Mikroanalytisches Laboratorium, 5251 Elbach über Engelskirchen, West Germany.

(9) It is noteworthy that the lower infrared energy range from 600 to 300 cm^{-1} (as well as the higher energy carbonyl stretching region) has proven to be valuable in a "fingerprinting" characterization of these and other kinds of organometallic carbonyl clusters produced in our laboratories. Infrared spectra (recorded as Nujol mulls on a Beckman IR-8 spectrometer) show that the $Co_3(CO)_9X$ (X = S, Se) molecules of C_{3v}-3*m* geometry contain two broad bands at ~500 (vs) and ~400 (s) cm^{-1} and that the $FeCo_2(CO)_9X$ (X = S, Se, Te) molecules of C_s-*m* geometry expectedly give rise to a complicated spectral pattern with at least six resolvable frequencies in the 600–300-cm^{-1} range.[7] Infrared spectra in hexane solution reveal that the terminal carbonyl stretching region contains eight detectable bands for the $FeCo_2(CO)_9X$ (X = S, Se, Te) molecules as compared with four observed for the $Co_3(CO)_9X$ (X = S, Se) molecules.[6,7]

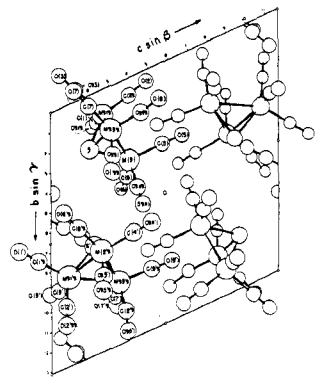

Figure 1. [100] projection of the primitive triclinic unit cell of $Co_3(CO)_9S$. There are two crystallographically independent molecules in this centrosymmetric cell.

Preliminary X-Ray and Esr Characterization. Weissenberg photographs of $Co_3(CO)_9Se$ and the isomorphous $FeCo_2(CO)_9Se$ revealed an interesting relationship between the crystal structure of $Co_3(CO)_9Se$ and that of $Co_3(CO)_9S$. While these compounds are not isomorphous, a triclinic unit cell can be chosen for $Co_3(CO)_9Se$ which is of nearly the same dimensions as that chosen by Wei and Dahl[4] for $Co_3(CO)_9S$. Based on this unit cell, the intensities of reflections of the type $\{hkl\}$ with $h + k = 2n$ in the photographs of $Co_3(CO)_9Se$ bear a marked similarity to those of $Co_3(CO)_9S$, but reflections of the type $\{hkl\}$ with $h + k = 2n + 1$ are completely absent, indicative of a *C*-centered cell. The implications of this relationship can be appreciated from an examination of the packing diagram of $Co_3(CO)_9S$ in Figure 1. It can be seen that if one of the two crystallographically independent molecules is rotated in such a way that the sulfur atom and one of the metal atoms are interchanged (*e.g.*, S′ and M(1′) in Figure 1), the two molecules exhibit an approximate *C*-centered relationship to each other. Since the packing of the molecules in the unit cell of $Co_3(CO)_9S$ appears to be controlled to a large extent by interactions between molecules related by a center of symmetry, it seemed a reasonable hypothesis that in the crystal transformation from $Co_3(CO)_9S$ to $Co_3(CO)_9Se$ one of the independent molecules of $Co_3(CO)_9S$ remains approximately in the same position with respect to the triclinic axes, while the other molecule is rotated into a position *C*-centered from the first one.

Before structural work was begun on these compounds, this crystal-packing hypothesis was tested by the use of single-crystal esr measurements to determine the orientation of the one crystallographically independent $Co_3(CO)_9Se$ molecule in the unit cell. Single crystals of $FeCo_2(CO)_9Se$ containing about 0.5% $Co_3(CO)_9Se$ were grown. These crystals were mounted on quartz rods and aligned by the use of X-ray oscillation photographs. The quartz rods then were attached to a Varian single-crystal goniometer and were carefully positioned in the microwave cavity of a conventional Varian E-3 esr spectrometer. The spectra obtained from these crystals at room temperature consist of a single broad line whose width and amplitude vary depending upon the orientation of the crystal with respect to the magnetic field. Since for a *C*-centered lattice the threefold axes of the one independent molecule of $Co_3(CO)_9Se$ and the other three symmetry-related molecules per cell are all parallel with one another, it follows that the paramagnetic $Co_3(CO)_9Se$ molecules doped into the isomorphous, diamagnetic $FeCo_2(CO)_9Se$ host should give rise to only one esr signal as experimentally observed. (In contrast, two overlapping esr signals were found[5] for a single crystal of $Co_3(CO)_9S$ doped into its isomorphous, diamagnetic $FeCo_2(CO)_9S$ host, owing to the threefold axes of the two crystallographically independent molecules per cell being much differently oriented in the crystals.) The orientation of the threefold axis of the independent $Co_3(CO)_9Se$ molecule in the unit cell was experimentally determined by rotation of the crystal to obtain the maximum amplitude and minimum peak width of the one observed signal. Since the crystal used in this study was in the form of a plate with the crystallographic *a* axis parallel to the two large opposite, parallel faces of the crystal, the crystal orientation of the threefold molecular axis was established by a rotation of the crystal about the normal to the large faces of the crystal and by a measurement of the angle between the *a* axis and the component of the threefold molecular axis in the plane of one

Table I. Orientations of the Two Crystallographically Independent Molecules of $FeCo_2(CO)_9S$ Compared with Orientation of the One Independent Molecule of $FeCo_2(CO)_9Se$[a]

	Angle,[b] deg	Angle,[c] deg
$FeCo_2(CO)_9S$		
Molecule I	90	52
Molecule II	51	15
$FeCo_2(CO)_9Se$	90 (3)	52 (2)

[a] As obtained from single-crystal esr measurements of $FeCo_2(CO)_9Se$ containing 0.5% $Co_3(CO)_9Se$. [b] Angle between the a axis and the component of the molecular threefold axis in the large face of the plate-like crystal. [c] Angle between the large face of the crystal and the component of the molecular threefold axis in the b^*–c^* plane.

that both $Co_3(CO)_9S$ and $Co_3(CO)_9Se$ have very nearly the same isotropic hyperfine coupling constants; a broadening of the individual hyperfine components observed in the single-crystal esr spectrum of $Co_3(CO)_9Se$ compared to that of $Co_3(CO)_9S$ presumably accounts for the lack of any resolved hyperfine structure in the solution esr spectrum of $Co_3(CO)_9Se$.

Low-Temperature Single-Crystal Esr Measurements. A single crystal of $FeCo_2(CO)_9Se$ containing about 0.5% $Co_3(CO)_9Se$ was mounted on a quartz rod with its a axis within 0.5° of the axis of the rod. The rod was then rotated to align the molecular threefold axis with the applied magnetic field. The resulting esr spectrum recorded at 77°K is shown in Figure 2. The hyperfine coupling constant obtained from this spectrum is 72.8 G, compared to a coupling constant of 74.3 G obtained from the $Co_3(CO)_9S$ spectrum. The considerably greater line widths of the 22 hyperfine components detected in the $Co_3(CO)_9Se$ spectrum compared with

Table II. Crystal Data for the $M_3(CO)_9X$ Compounds

	a, Å	b, Å	c, Å	α, deg	β, deg	γ, deg
$Co_3(CO)_9S$[4]	9.67 (2)	13.23 (3)	13.41 (3)	110.0 (2)	108.3 (2)	97.3 (2)
$FeCo_2(CO)_9S$[1]	9.56 (2)	13.12 (2)	13.38 (2)	109.8 (2)	107.5 (2)	97.5 (2)
$Co_3(CO)_9Se$	9.5030 (5)	13.9184 (9)	14.1229 (8)	114.3171 (2)	117.752 (2)	84.556 (3)
$FeCo_2(CO)_9Se$	9.4595 (4)	13.8419 (6)	14.0908 (6)	114.005 (1)	117.660 (1)	84.608 (2)
$FeCo_2(CO)_9Te$	8.773 (16)	15.205 (29)	14.578 (28)	117.29 (5)	118.73 (5)	78.42 (6)

	Space group	Z	Vol, Å^3	d_{calcd}, g/cm^3	d_{obsd},[a] g/cm^3	μ, cm^{-1}	n[b]	m[c]	R_1	R_2	e[d]
$Co_3(CO)_9S$[4]	$P\bar{1}$	4	1476	2.08	2.00						
$FeCo_2(CO)_9S$[1]	$P\bar{1}$	4	1454	2.09	2.05						
$Co_3(CO)_9Se$	$C\bar{1}$	4	1492	2.26	2.20	60.1	48	1370	0.043	0.049	1.1
$FeCo_2(CO)_9Se$	$C\bar{1}$	4	1482	2.26	2.20	58.5	48	1643	0.030	0.034	1.4
$FeCo_2(CO)_9Te$	$C\bar{1}$	4	1509	2.44	2.40	51.3	22	1554	0.023	0.025	1.4

[a] d_{obsd} = density measured by flotation. [b] n = number of reflections used in the calculation of lattice parameters. [c] m = number of reflections used in least-squares refinement. [d] e = standard deviation of a reflection of unit weight.

of the faces. The crystal was then remounted about the a axis and the angle measured between the component of the threefold axis in the b^*–c^* plane and the same large crystal face. Finally, a Weissenberg photograph of the crystal mounted about the a axis was used to determine the angles between b^*, c^*, and this large crystal face. It was found that this face of the crystal makes an angle of 81° (2) with the $-c^*$ axis and an angle of 33° (2) with the b^* axis. The observed angles were then compared to those calculated for the two molecules in the structure of $FeCo_2(CO)_9S$ (Table I). These measurements indicate that within experimental error

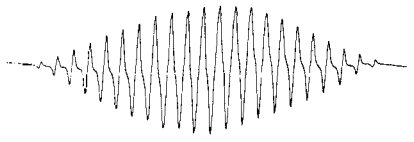

Figure 2. The esr spectrum of a single crystal of diamagnetic $FeCo_2(CO)_9Se$ doped with about 0.5% of paramagnetic $Co_3(CO)_9Se$. This spectrum containing 22 hyperfine components was recorded at 77°K with the molecular threefold axis parallel to the magnetic field direction.

the molecules in $Co_3(CO)_9Se$ are oriented in the same way with respect to the crystallographic axes as the unprimed molecule (molecule I) in the crystal packing diagram of $Co_3(CO)_9S$ (Figure 1).

Solution of Esr Spectrum of $Co_3(CO)_9Se$. Measurements of the esr spectrum of $Co_3(CO)_9Se$ in saturated hexane and ether solutions showed a single broad line which appears to be independent of solvent and temperature and which gives only the expected loss of intensity upon dilution. It was initially expected that the solution spectrum would show a hyperfine structure due to the interaction of the unpaired electron with all three cobalt nuclei ($I = {}^7/_2$ for ^{59}Co, 100%). While the predicted 22 hyperfine components are partially resolved in the solution esr spectrum of $Co_3(CO)_9S$, they are not at all resolvable in the corresponding spectrum of the selenium analog. A superposition of these two spectra, however, indicates those found in the $Co_3(CO)_9S$ spectrum are probably a consequence of the larger spin–orbit coupling constant of the selenium atom. There is no discernible evidence of any resolvable splitting of each hyperfine component as a result of hyperfine interaction with the ^{77}Se nucleus (7.58% abundance; $I = {}^1/_2$); a small unresolvable splitting would contribute to the larger observed line widths of the hyperfine components.

Single-Crystal X-Ray Data and Data Collection. The crystal data for the $M_3(CO)_9X$ compounds are summarized in Table II. Small well-shaped crystals of $Co_3(CO)_9Se$, $FeCo_2(CO)_9Se$, and $FeCo_2(CO)_9Te$ were chosen for X-ray structural determinations. Each crystal was mounted in turn on a General Electric four-angle automated diffractometer, and a complete sphere of intensity data was collected to $2\theta = 45°$ with Mo Kα radiation at room temperature (~22°). A θ–2θ scan technique was used, and background was measured for 10 sec on each side of the peak. In the case of $FeCo_2(CO)_9Se$ the crystal was mounted about the crystallographic a axis, while in the other two cases the crystals were mounted about the [$\bar{1}$10] direction. During the data collection from the $Co_3(CO)_9Se$ crystal a small decay in the intensity of a set of periodically measured standard reflections was observed which necessitated a correction to the observed intensities. A Lorentz-polarization correction was applied and a structure factor F calculated for each reflection. A $\sigma(F)$ was assigned to each reflection from the formulas $\sigma(F) = \sigma(F^2)/2F$ and $\sigma(F^2) = [S + (T_S/T_B)^2B + 0.001I^2]^{1/2}$, where S is the total integrated scan count, B is the background count, T_S and T_B are the scan and background count times, and $I = S + (T_S/T_B)B$. All reflections with $F < 6\sigma(F)$ were considered unobserved and were omitted from further consideration.

The crystals of $FeCo_2(CO)_9Se$ and $Co_3(CO)_9Se$ selected for data collection were approximately equidimensional blocks with an average side dimension of 0.13 mm. Trial absorption corrections[10] for selected reflections (which produced the extreme values of absorption corrections) from these crystals indicated for each of these two selenium compounds that the absorption correction was comparable to the random error in the intensities (with transmission

(10) J. F. Blount, DEAR, an absorption correction program based on the methods of W. R. Busing and H. A. Levy, *Acta Crystallogr.* 10, 180 (1957).

coefficients ranging from 0.57 to 0.61); consequently, no absorption correction was applied to the X-ray intensity data of $FeCo_2(CO)_9Se$ and $Co_3(CO)_9Se$. The crystal of $FeCo_2(CO)_9Te$ chosen for data collection had dimensions 0.08 × 0.02 × 0.18 mm, which gave transmission factors ranging from 0.58 to 0.69; therefore, in this case an absorption correction was applied.[10] The linear absorption coefficients for the three compounds are tabulated in Table II. No corrections for extinction were made.

The lattice parameters for these compounds (Table II) were calculated with a least-squares program[11] that fitted the 2θ, χ, and ϕ values of a number of reflections centered by the use of a top-bottom-left-right technique with Mo Kα radiation at room temperature (λ 0.71069 Å). A takeoff angle of 2° was used for both lattice parameter measurements and data collection; in all of these experiments, collimators of 1-mm diameter were utilized together with a 0.002-in. zirconium filter. Because of the large number of reflections used in the determination of the lattice parameters of $Co_3(CO)_9Se$ and $FeCo_2(CO)_9Se$, the estimated standard deviations obtained from the least-squares fits are unrealistically small.

Structural Determinations and Refinements of $Co_3(CO)_9Se$, $FeCo_2(CO)_9Se$, and $FeCo_2(CO)_9Te$. The positions of the selenium atom and the three metal atoms of $FeCo_2(CO)_9Se$ were obtained from the interpretation of a three-dimensional Patterson map.[12] These coordinates were then used to position a rigid-body model of the molecule in the unit cell. This model was constructed from the average interatomic distances and angles obtained by Stevenson, Wei, and Dahl[1] for $FeCo_2(CO)_9S$. A least-squares refinement was then carried out in which the positional parameters of the crystallographically independent molecule were constrained to exact C_{3v} symmetry.[13,14] This noncrystallographic constraint lowers the number of independent positional parameters from 66 to only 18 (*i.e.*, consisting of 6 orientation parameters and 12 distortion coordinates). Application of this least-squares model together with the use of individual isotropic temperature factors for the 22 atoms of $FeCo_2(CO)_9Se$ resulted in convergence of the refinement to $R_1 = [\Sigma||F_o| - |F_c||/\Sigma|F_o|] = 0.069$ and $R_2 = [\Sigma w||F_o| - |F_c||^2/\Sigma w|F_o|^2]^{1/2} = 0.061$, with a metal–metal distance of 2.576 Å and a metal–selenium distance of 2.287 Å. The C_{3v} constraint was then broken, and the refinement continued with 66 positional parameters and 22 isotropic temperature factors. This unconstrained refinement converged to $R_1 = 0.055$ and $R_2 = 0.040$. Application of Hamilton's *R*-factor ratio test[15] indicated a deviation from C_{3v} symmetry at the 0.005 significance level. The differences in the atomic coordinates obtained from these two refinements were then calculated; it was observed that the shift of the selenium atomic position was 0.01 Å, the largest metal shift was 0.02 Å, the largest carbon shift was 0.10 Å, and the largest oxygen shift was 0.18 Å. It was also noted that while the final metal–metal distances varied by as much as 4σ from the mean, the metal–metal distance obtained from the constrained C_{3v} refinement was within 1σ of the mean. Details of this refinement technique applied to the $FeCo_2(CO)_9Se$ molecule are given elsewhere by one of us.[13] It should be noted that such a refinement allows the application of chemically reasonable constraints to a system whose bond lengths and angles are not sufficiently well known (as in the case of the $FeCo_2(CO)_9Se$ complex) to justify a completely constrained rigid-body refinement. In addition to a large reduction of the number of parameters to be refined (which greatly decreases the computer costs due to much less calculation time), this symmetry-flexible rigid-group least-squares model retains the increased rate and range of convergence inherent in a standard rigid-group refinement.[16]

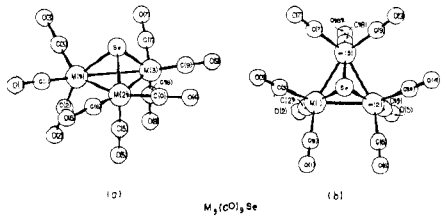

Figure 3. Basic molecular geometry of the $Co_3(Co)_9Se$ and $FeCo_2(CO)_9Se$ molecules.

Anisotropic temperature factors for all atoms and corrections for anomalous dispersion[17,18] were then introduced for the $FeCo_2(CO)_9Se$ molecule, and the nonconstrained refinement was allowed to converge to a final $R_1 = 0.030$ and $R_2 = 0.034$. The refinements of $Co_3(CO)_9Se$ and $FeCo_2(CO)_9Te$ were carried out in a similar manner.

In all of these refinements the scattering factor tables of Hanson, *et al.*,[19] were used along with the real and imaginary anomalous dispersion corrections.[17,18] The function minimized in the refinements was $\Sigma w||F_o| - |F_c||^2$, where the weights were assigned according to the estimated standard deviations of the observed structure factors. Final Fourier difference maps from the refinements showed no residual peaks greater than 0.6 e/Å^3.

Positional and thermal parameters from the output of the last least-squares cycles are tabulated in Table III.[20] Distances and angles calculated with the ORFFE program[21] are given in Table IV. The full inverse matrix of the last least-squares cycle for each complex was used in the error calculations, which included the effect of the estimated uncertainties in the unit cell parameters.

Results and Discussion

General Description of the Molecular and Crystal Structures. The basic molecular geometry (Figure 3) of $Co_3(CO)_9Se$, $FeCo_2(CO_9)Se$, and $FeCo_2(CO)_9Te$ is analogous to that of $Co_3(CO)_9S$ and $FeCo_2(CO)_9S$. Its trinuclear metal architecture may be described as a tetrahedrally shaped M_3X cluster system formed by the symmetrical coordination of an apical chalcogen atom X to a basal $M_3(CO)_9$ fragment containing three $M(CO)_3$ groups situated at the corners of an equilateral triangle and linked to one another by metal–metal bonds. The idealized configuration of $Co_3(CO)_9Se$ (as well as that of $Co_3(CO)_9S$) possesses C_{3v}-3*m* point group symmetry. This trigonal molecular symmetry is expectedly reduced to C_s-*m* by the formal substitution of an iron atom in place of one cobalt atom to give the $FeCo_2(CO)_9X$ complexes (X = S, Se, Te). Owing to the crystal-disordered model assumed in each of these iron dicobalt carbonyl chalcogen complexes, the resulting disorder-averaged configuration (containing a statistical distribution of the one iron and two cobalt atoms averaged over

(11) A. S. Foust, "ANGSET," Ph.D. Thesis, University of Wisconsin, Madison, Jan 1970.

(12) J. F. Blount, "A Three-Dimensional Crystallographic Fourier Summation Program for the CDC Computer," Ph.D. Thesis, University of Wisconsin, Madison, 1965.

(13) C. E. Strouse, *Acta Crystallogr., Sect. A*, 26, 604 (1970).

(14) As previously utilized in the least-squares refinement of $FeCo_2(CO)_9S$,[1] a crystal-disordered model was likewise employed in the least-squares refinements of $FeCo_2(CO)_9Se$ and $FeCo_2(CO)_9Te$; this model assumes a statistical distribution of the one iron and two cobalt atoms over the three metal positions in the crystallographically independent molecule. Such a crystal disordering, which was anticipated in view of the nearly identical covalent radii of iron (1.165 Å) and cobalt (1.157 Å), is not incompatible with the equivalent metal–metal distances determined in the $FeCo_2(CO)_9X$ complexes (X = S, Se, Te).

(15) W. C. Hamilton, *Acra Crystallogr.*, 18, 502 (1965).

(16) For a general description together with applications of standard rigid-body least-squares refinement, see (a) C. Scheringer, *ibid.*, 16, 546 (1963); (b) S. J. LaPlaca and J. A. Ibers, *ibid.*, 18, 511 (1965), and references contained therein; (c) R. J. Doedens and L. F. Dahl, *J. Amer. Chem. Soc.*, 88, 4847 (1966), and references contained therein.

(17) For Mo Kα radiation the values of the dispersion corrections to the atomic scattering factors are $\Delta f' = -0.5$, $\Delta f'' = 2.2$ for Te; $\Delta f' = -0.1$, $\Delta f'' = 2.4$ for Se; $\Delta f' = 0.4$, $\Delta f'' = 1.1$ for Co; $\Delta f' = 1.1$, $\Delta f'' = 1.0$ for Fe.[18]

(18) "International Tables for X-Ray Crystallography," Vol. III, Kynoch Press, Birmingham, England, 1962, p 215.

(19) H. P. Hanson, F. Herman, J. D. Lea, and S. Skillman, *Acta Crystallogr.*, 17, 1040 (1964).

(20) Calculated and observed structure factors will appear following these pages in the microfilm edition of this volume of the journal. Single copies may be obtained from the Reprint Department, ACS Publications, 1155 Sixteenth St., N.W., Washington, D. C. 20036, by referring to author, title of article, volume, and page number. Remit check or money order for $3.00 for photocopy or $2.00 for microfiche.

(21) W. R. Busing, K. O. Martin, and H. A. Levy, "ORFFE, A Fortran Crystallographic Function and Error Program," ORNL-TM-306, Oak Ridge National Laboratory, 1964.

Table III. Final Atomic Parameters[a,b]

	Positional parameters for $Co_3(CO)_6X$ (X = Se)			Positional parameters for $FeCo_2(CO)_9X$ (X = Se)			Positional parameters for $FeCo_2(CO)_9X$ (X = Te)		
	x	*y*	*z*	*x*	*y*	*z*	*x*	*y*	*z*
X	0.2402 (1)	0.1545 (1)	0.1157 (1)	0.23965 (8)	0.15571 (5)	0.11398 (5)	0.52920 (5)	0.26829 (3)	0.10294 (3)
M(2)	0.3124 (2)	0.2659 (1)	0.3072 (1)	0.31369 (10)	0.26397 (6)	0.30637 (8)	0.64834 (10)	0.38184 (6)	0.30979 (6)
M(3)	0.4852 (2)	0.1243 (1)	0.2359 (1)	0.48435 (10)	0.12435 (7)	0.23568 (8)	0.84876 (10)	0.28188 (6)	0.21311 (6)
M(1)	0.2122 (2)	0.0639 (1)	0.2100 (1)	0.21385 (10)	0.06453 (7)	0.20987 (8)	0.66199 (10)	0.19073 (6)	0.23945 (7)
C(5)	0.4089 (15)	0.2801 (10)	0.4563 (12)	0.4086 (9)	0.2791 (5)	0.4551 (7)	0.8097 (9)	0.4126 (4)	0.4570 (6)
O(5)	0.4712 (13)	0.2903 (8)	0.5507 (8)	0.4692 (7)	0.2913 (4)	0.5512 (5)	0.9081 (6)	0.4363 (4)	0.5516 (4)
C(8)	0.6105 (15)	0.1191 (10)	0.3725 (12)	0.6110 (8)	0.1202 (5)	0.3749 (7)	1.0360 (8)	0.3025 (4)	0.3476 (5)
O(8)	0.6996 (11)	0.1155 (8)	0.4615 (8)	0.6986 (6)	0.1161 (5)	0.4629 (5)	1.1590 (6)	0.3157 (4)	0.4315 (4)
C(2)	0.2963 (13)	0.0493 (9)	0.3479 (11)	0.2951 (8)	0.0506 (5)	0.3475 (6)	0.8194 (9)	0.1946 (4)	0.3755 (6)
O(2)	0.3434 (11)	0.0404 (7)	0.4322 (8)	0.3413 (7)	0.0410 (4)	0.4317 (5)	0.9195 (7)	0.1923 (4)	0.4622 (4)
C(6)	0.1221 (14)	0.3126 (10)	0.2932 (12)	0.1274 (9)	0.3151 (5)	0.2951 (6)	0.4583 (9)	0.4031 (5)	0.3316 (6)
O(6)	0.0057 (11)	0.3460 (7)	0.2842 (9)	0.0100 (7)	0.3483 (4)	0.2867 (5)	0.3375 (7)	0.4202 (4)	0.3473 (5)
C(4)	0.4116 (16)	0.3824 (11)	0.3278 (13)	0.4097 (9)	0.3811 (6)	0.3269 (7)	0.6510 (8)	0.4944 (5)	0.3014 (5)
O(4)	0.4679 (13)	0.4577 (8)	0.3402 (10)	0.4684 (7)	0.4561 (5)	0.3404 (6)	0.6497 (7)	0.5672 (4)	0.2948 (4)
C(9)	0.6130 (17)	0.2198 (11)	0.2396 (13)	0.6104 (9)	0.2181 (6)	0.2398 (7)	0.8945 (8)	0.3745 (4)	0.1853 (5)
O(9)	0.6854 (12)	0.2788 (8)	0.2415 (10)	0.6859 (7)	0.2774 (5)	0.2414 (6)	0.9251 (7)	0.4329 (4)	0.1677 (4)
C(7)	0.5148 (16)	−0.0009 (12)	0.1379 (12)	0.5156 (9)	0.0002 (6)	0.1384 (7)	0.9110 (8)	0.1721 (5)	0.1168 (6)
O(7)	0.5333 (14)	−0.0783 (8)	0.0759 (10)	0.5380 (8)	−0.0776 (5)	0.0786 (5)	0.9515 (7)	0.1041 (4)	0.0567 (4)
C(3)	0.1897 (15)	−0.0733 (11)	0.1074 (11)	0.1916 (8)	−0.0729 (6)	0.1096 (6)	0.6867 (8)	0.0649 (5)	0.1472 (6)
O(3)	0.1768 (12)	−0.1586 (8)	0.0432 (9)	0.1778 (6)	−0.1581 (4)	0.0453 (5)	0.7026 (7)	−0.0145 (4)	0.0897 (5)
C(1)	0.0052 (16)	0.0756 (9)	0.1817 (10)	0.0075 (9)	0.0753 (5)	0.1819 (6)	0.4678 (9)	0.1764 (5)	0.2439 (6)
O(1)	−0.1239 (10)	0.0808 (7)	0.1635 (8)	−0.1214 (6)	0.0815 (4)	0.1634 (4)	0.3453 (7)	0.1696 (4)	0.2481 (6)

	Anisotropic temperature factors for $Co_3(CO)_9X$ (X = Se)						Anisotropic temperature factors for $FeCo_2(CO)_9X$ (X = Se)						Anisotropic temperature factors for $FeCo_2(CO)_9X$ (X = Te)					
	10^4B_{11}	10^4B_{22}	10^4B_{33}	10^4B_{12}	10^4B_{13}	10^4B_{23}	10^4B_{11}	10^4B_{22}	10^4B_{33}	10^4B_{12}	10^4B_{13}	10^4B_{23}	10^4B_{11}	10^4B_{22}	10^4B_{33}	10^4B_{12}	10^4B_{13}	10^4B_{23}
X	134 (2)	65 (1)	61 (1)	11 (1)	45 (1)	34 (1)	136 (1)	61 (1)	61 (1)	13 (1)	40 (1)	30 (1)	118 (1)	53 (1)	55 (1)	−2 (1)	17 (1)	23 (1)
M(2)	121 (3)	48 (1)	76 (2)	6 (1)	53 (2)	26 (1)	121 (1)	42 (1)	73 (1)	8 (1)	48 (1)	20 (1)	134 (2)	41 (1)	62 (1)	5 (1)	46 (1)	18 (1)
M(3)	111 (3)	59 (1)	79 (2)	12 (1)	57 (2)	33 (1)	108 (1)	53 (1)	78 (1)	13 (1)	52 (1)	28 (1)	112 (1)	43 (1)	54 (1)	2 (1)	36 (1)	20 (1)
M(1)	107 (2)	47 (1)	67 (2)	5 (1)	45 (2)	26 (1)	104 (1)	41 (1)	64 (1)	4 (1)	39 (1)	19 (1)	132 (2)	42 (1)	77 (1)	−2 (1)	41 (1)	28 (1)
C(5)	159 (25)	56 (10)	81 (14)	−13 (13)	42 (16)	20 (10)	159 (14)	47 (5)	96 (8)	12 (7)	57 (9)	23 (6)	203 (14)	45 (4)	91 (7)	20 (6)	89 (9)	20 (4)
O(5)	320 (25)	102 (9)	82 (10)	3 (12)	75 (14)	35 (8)	324 (14)	85 (5)	89 (6)	20 (6)	71 (8)	32 (4)	253 (11)	99 (4)	65 (4)	17 (6)	30 (6)	21 (3)
C(8)	115 (23)	78 (12)	95 (15)	0 (13)	57 (15)	31 (11)	130 (13)	50 (5)	117 (9)	10 (7)	77 (9)	32 (6)	143 (12)	58 (4)	64 (6)	2 (6)	50 (8)	24 (4)
O(8)	172 (19)	125 (10)	111 (11)	6 (11)	33 (12)	67 (9)	192 (11)	128 (6)	129 (7)	13 (6)	40 (7)	78 (5)	180 (10)	98 (4)	80 (4)	−8 (5)	19 (6)	40 (4)
C(2)	120 (21)	43 (9)	76 (13)	−1 (11)	44 (14)	16 (9)	110 (11)	51 (5)	76 (7)	0 (6)	43 (7)	22 (5)	174 (14)	52 (4)	100 (7)	−3 (6)	62 (9)	28 (5)
O(2)	239 (20)	124 (10)	99 (10)	18 (11)	65 (12)	79 (9)	225 (11)	107 (5)	88 (6)	8 (6)	49 (7)	58 (5)	240 (12)	122 (5)	105 (5)	4 (6)	47 (7)	70 (4)
C(6)	119 (23)	75 (12)	113 (15)	12 (13)	57 (16)	58 (11)	180 (14)	47 (5)	109 (8)	8 (7)	83 (9)	29 (5)	202 (14)	61 (5)	104 (7)	10 (7)	76 (9)	34 (5)
O(6)	205 (20)	88 (8)	161 (13)	43 (11)	103 (14)	60 (8)	191 (11)	83 (5)	173 (7)	48 (6)	110 (8)	50 (5)	253 (12)	120 (5)	207 (8)	42 (6)	176 (8)	67 (5)
C(4)	200 (28)	63 (12)	155 (19)	12 (15)	116 (19)	40 (12)	173 (14)	56 (6)	124 (9)	16 (7)	86 (9)	30 (6)	165 (13)	51 (5)	65 (6)	12 (6)	52 (7)	21 (4)
O(4)	312 (25)	81 (9)	234 (17)	−14 (12)	161 (17)	63 (10)	305 (15)	73 (5)	231 (9)	−10 (7)	134 (10)	68 (6)	298 (13)	59 (3)	136 (6)	15 (5)	89 (7)	48 (4)
C(9)	243 (31)	59 (11)	157 (19)	29 (15)	133 (21)	47 (12)	173 (15)	80 (7)	128 (9)	38 (8)	96 (10)	53 (6)	155 (13)	53 (4)	74 (6)	2 (6)	51 (7)	17 (4)
O(9)	274 (23)	112 (11)	239 (17)	8 (12)	181 (17)	89 (11)	265 (13)	114 (6)	232 (9)	10 (7)	174 (9)	84 (6)	309 (13)	78 (4)	120 (5)	−29 (6)	86 (7)	47 (4)
C(7)	158 (25)	105 (14)	90 (15)	−1 (15)	76 (17)	47 (12)	174 (15)	87 (7)	124 (9)	36 (8)	104 (10)	48 (7)	175 (13)	62 (5)	77 (6)	6 (6)	40 (8)	32 (5)
O(7)	381 (28)	96 (10)	165 (14)	45 (13)	187 (17)	42 (10)	343 (15)	85 (5)	166 (8)	50 (7)	173 (9)	30 (5)	368 (14)	75 (4)	102 (5)	49 (6)	115 (7)	19 (3)
C(3)	130 (23)	86 (13)	84 (14)	25 (14)	57 (15)	42 (11)	159 (13)	60 (6)	82 (7)	17 (7)	54 (8)	27 (5)	152 (13)	63 (5)	110 (8)	1 (7)	39 (8)	41 (5)
O(3)	243 (21)	68 (8)	154 (13)	18 (11)	98 (14)	26 (9)	236 (12)	55 (4)	140 (7)	18 (6)	78 (7)	10 (4)	309 (14)	55 (3)	151 (6)	3 (6)	71 (8)	15 (4)
C(1)	174 (26)	64 (11)	71 (13)	−2 (14)	65 (16)	28 (9)	165 (14)	53 (5)	64 (7)	4 (7)	52 (8)	17 (5)	192 (14)	61 (5)	138 (8)	0 (7)	76 (9)	51 (5)
O(1)	115 (16)	94 (8)	128 (11)	11 (10)	55 (11)	44 (8)	130 (9)	104 (5)	115 (6)	10 (5)	58 (6)	35 (4)	246 (12)	110 (5)	256 (9)	0 (6)	156 (9)	87 (5)

[a] Estimated standard deviation of the last significant figure is given in parentheses. [b] Anisotropic temperature factors are of the form $\exp[-(\beta_{11}h^2 + B_{22}k^2 + B_{33}l^2 + 2B_{12}hk + 2B_{13}hl + 2B_{23}kl)]$.

Table IV. Intramolecular Distances (Å) and Angles (Deg) for $M_3(CO)_9X$

	$FeCo_2(CO)_9Se$	$Co_3(CO)_9Se$	$FeCo_2(CO)_9Te$
	A. Bond Lengths		
M–M			
M(1)–M(2)	2.570 (1)	2.609 (2)	2.599 (6)
M(2)–M(3)	2.583 (1)	2.624 (2)	2.595 (4)
M(3)–M(1)	2.580 (1)	2.616 (2)	2.600 (4)
M–X			
M(1)–X	2.287 (1)	2.283 (2)	2.466 (4)
M(2)–X	2.283 (1)	2.283 (2)	2.467 (5)
M(3)–X	2.284 (1)	2.281 (2)	2.466 (4)
M–C			
M(1)–C(1)	1.808 (8)	1.821 (13)	1.795 (8)
M(1)–C(3)	1.809 (7)	1.818 (15)	1.808 (8)
M(2)–C(4)	1.786 (8)	1.802 (14)	1.776 (8)
M(2)–C(6)	1.797 (8)	1.811 (13)	1.784 (7)
M(3)–C(7)	1.812 (8)	1.820 (15)	1.810 (8)
M(3)–C(9)	1.809 (8)	1.854 (15)	1.794 (8)
M(1)–C(2)	1.811 (8)	1.823 (13)	1.771 (8)
M(2)–C(5)	1.781 (8)	1.792 (14)	1.804 (8)
M(3)–C(8)	1.784 (8)	1.761 (14)	1.785 (7)
C–O			
C(1)–O(1)	1.125 (7)	1.133 (12)	1.133 (8)
C(3)–O(3)	1.131 (7)	1.133 (14)	1.139 (8)
C(4)–O(4)	1.127 (8)	1.133 (14)	1.151 (7)
C(6)–O(6)	1.134 (7)	1.130 (13)	1.145 (8)
C(7)–O(7)	1.139 (8)	1.136 (15)	1.133 (7)
C(9)–O(9)	1.124 (8)	1.106 (14)	1.138 (7)
C(2)–O(2)	1.119 (7)	1.116 (12)	1.154 (8)
C(5)–O(5)	1.141 (8)	1.127 (13)	1.141 (8)
C(8)–O(8)	1.150 (8)	1.162 (13)	1.138 (7)
M–M–M			
M(2)–M(3)–M(1)	59.71 (3)	59.72 (6)	60.05 (13)
M(1)–M(2)–M(3)	60.08 (3)	59.98 (6)	60.07 (7)
M(3)–M(1)–M(2)	60.21 (3)	60.30 (6)	59.88 (11)
M–X–M			
M(2)–X–M(1)	68.44 (4)	69.70 (6)	63.59 (16)
M(1)–X–M(3)	68.71 (4)	69.94 (6)	63.62 (7)
M(3)–X–M(2)	68.88 (4)	70.21 (6)	63.47 (8)
X–M–M			
X–M(2)–M(3)	55.58 (3)	54.86 (6)	58.25 (12)
X–M(2)–M(1)	55.85 (3)	55.16 (6)	58.18 (8)
X–M(3)–M(2)	55.54 (3)	54.93 (6)	58.28 (14)
X–M(3)–M(1)	55.69 (3)	55.07 (6)	58.18 (12)
X–M(1)–M(2)	55.72 (3)	55.14 (6)	58.22 (12)
X–M(1)–M(3)	55.60 (3)	54.99 (6)	58.19 (11)
C–M–C			
C(5)–M(2)–C(6)	99.9 (3)	100.9 (6)	98.5 (3)
C(5)–M(2)–C(4)	99.0 (3)	99.3 (6)	99.7 (3)
C(8)–M(3)–C(9)	99.7 (3)	100.2 (6)	98.4 (3)
C(8)–M(3)–C(7)	100.7 (3)	99.9 (6)	100.6 (3)
C(2)–M(1)–C(3)	100.3 (3)	100.4 (6)	99.8 (3)
C(2)–M(1)–C(1)	98.8 (3)	99.8 (6)	99.8 (3)
C(6)–M(2)–C(4)	96.8 (3)	99.6 (6)	97.8 (3)
C(9)–M(3)–C(7)	100.5 (3)	100.9 (6)	100.1 (3)
C(3)–M(1)–C(1)	98.9 (3)	99.4 (6)	100.3 (3)
M–C–O			
M(2)–C(6)–O(6)	178.6 (7)	176.5 (11)	177.6 (6)
M(2)–C(4)–O(4)	178.7 (7)	177.0 (13)	178.8 (6)
M(3)–C(9)–O(9)	178.5 (7)	177.7 (13)	179.3 (6)
M(3)–C(7)–O(7)	178.7 (8)	179.1 (13)	179.1 (6)
M(1)–C(3)–O(3)	178.5 (7)	179.2 (12)	179.5 (7)
M(1)–C(1)–O(1)	179.3 (6)	178.7 (11)	178.5 (6)
M(2)–C(5)–O(5)	178.4 (6)	179.9 (12)	176.8 (6)
M(3)–C(8)–O(8)	176.5 (6)	176.6 (11)	177.5 (5)
M(1)–C(2)–O(2)	178.1 (6)	177.9 (11)	176.6 (6)
C–M–M			
C(5)–M(2)–M(3)	97.5 (2)	96.5 (4)	97.0 (2)
C(5)–M(2)–M(1)	97.2 (2)	96.3 (4)	96.7 (2)
C(8)–M(3)–M(2)	95.8 (2)	96.7 (4)	93.5 (2)
C(8)–M(3)–M(1)	97.8 (2)	97.8 (4)	96.2 (2)
C(2)–M(1)–M(2)	94.9 (2)	95.5 (3)	94.9 (2)
C(2)–M(1)–M(3)	96.5 (2)	96.0 (4)	97.1 (2)
C(6)–M(2)–M(3)	153.7 (2)	152.1 (4)	155.6 (2)
C(4)–M(2)–M(1)	155.8 (2)	155.2 (4)	154.2 (2)
C(7)–M(3)–M(2)	154.9 (2)	154.5 (4)	153.9 (2)
C(9)–M(3)–M(1)	150.7 (2)	150.5 (4)	155.4 (2)
C(3)–M(1)–M(2)	154.7 (2)	153.9 (4)	155.7 (2)
C(1)–M(1)–M(3)	154.9 (2)	154.5 (4)	151.7 (2)
C(4)–M(2)–M(3)	99.8 (2)	99.0 (4)	98.1 (2)
C(6)–M(2)–M(1)	98.1 (2)	96.2 (4)	99.3 (2)
C(9)–M(3)–M(2)	95.1 (2)	95.0 (4)	90.3 (2)
C(7)–M(3)–M(1)	99.1 (2)	98.7 (4)	96.4 (3)
C(1)–M(1)–M(2)	98.6 (2)	98.1 (4)	96.1 (2)
C(3)–M(1)–M(3)	97.7 (2)	97.3 (4)	98.9 (3)
X–M–C			
X–M(2)–C(6)	100.9 (2)	100.5 (4)	100.7 (2)
X–M(2)–C(4)	102.5 (2)	102.9 (5)	99.6 (2)
X–M(3)–C(9)	98.6 (2)	99.0 (5)	100.6 (2)
X–M(3)–C(7)	102.4 (2)	102.5 (4)	100.9 (2)
X–M(1)–C(3)	102.6 (2)	102.0 (4)	101.6 (3)
X–M(1)–C(1)	102.3 (2)	102.4 (4)	97.5 (2)
X–M(2)–C(5)	147.9 (2)	145.9 (4)	150.5 (2)
X–M(3)–C(8)	147.2 (2)	146.9 (4)	148.1 (2)
X–M(1)–C(2)	145.9 (2)	145.2 (3)	149.4 (2)

the three metal positions) also conforms experimentally to C_{3v} symmetry.[14]

The crystalline arrangement of the molecules of the virtually isomorphous $Co_3(CO)_9Se$ and $FeCo_2(CO)_9Se$ compounds is shown in Figure 4. Comparison of this figure with Figure 1 illustrates the validity of the particular interelationship (*vide supra*) between the crystal packing of these two selenium compounds and that of the $Co_3(Co)_9S$ and $FeCo_2(CO)_9S$ compounds (which are isomorphous) as correctly deduced from the single crystal esr and preliminary X-ray measurements. While X-ray photographs of the $FeCo_2(CO)_9Te$ compound indicate that it is isomorphous with both $M_3(CO)_9Se$ compounds, Figure 5 emphasizes that the crystal packing of the four $FeCo_2(CO)_9Te$ molecules in the unit cell is significantly different from that of the selenium analog. For the $Co_3(CO)_9Se$, $FeCo_2(CO)_9Se$, and $FeCo_2(CO)_9Te$ compounds (as also previously found for the $Co_3(CO)_9S$ and $FeCo_2(CO)_9S$ compounds), the experimental observation that the intermolecular O···O and O···C contacts are all greater than 2.9 and 3.2 Å, respectively, offers strong support for the premise that packing effects on the molecular geometries (*i.e.*, particularly the bond lengths) of these complexes are *negligible*. Substantial weight for this premise is also given by the relatively small degree of angular distortion of the carbonyl groups from linearity; all M–C–O bond angles (listed in Table IV for each of the three compounds) are within 4° of being linear.[22,23]

Stereochemical Interrelationships Based on X-Ray Diffraction Data. A comparison of the detailed molecular parameters of the entire series of compounds $FeCo_2(CO)_9X$ (X = S, Se, Te), and $Co_3(CO)_9X$ (X = S, Se) in Table V accents several stereochemical and bonding principles of significance with regard to metal

(22) It is noteworthy that nonlinear M–C–O bond angles in a $M(CO)_3$ group may be attributed to π-bonding as well as steric and packing effects.[23]

(23) S. F. A. Kettle, *Inorg. Chem.*, **4**, 1661 (1965); *J. Chem. Soc. A*, 421 (1966).

Table V. A Comparison of Molecular Parameters of $M_3(CO)_9X$ Compounds

	$FeCo_2(CO)_9S$[1]	$Co_3(CO)_9S$[4]	$FeCo_2(CO)_9Se$	$Co_3(CO)_9Se$	$FeCo_2(CO)_9Te$
M–M distance[a]	2.554 (3)	2.637 (3)	2.577 (1)	2.616 (1)	2.598 (2)
M–X–M angle[a]	72.6 (1)	76.1 (1)	68.7 (1)	69.9 (1)	63.6 (1)
M–X distance[a]	2.159 (4)	2.139 (4)	2.285 (1)	2.282 (1)	2.466 (1)
		X = S		X = Se	
M–M difference[b]		0.083 (4)		0.039 (1)	
M–X difference[b]		0.020 (6)		0.003 (1)	

[a] Average value. [b] Difference in M–M or M–X distance between $FeCo_2(CO)_9X$ and $Co_3(CO)_9X$. Standard deviations of the differences were calculated as $\sigma(A - B) = [\sigma(A)^2 + \sigma(B)^2]^{1/2}$.

cluster systems. One prominent structural feature which emerges from this systematic investigation is that, analogous to an average metal–metal bond-length shortening of 0.083 (4) Å observed upon formal replacement of one of the cobalt atoms of $Co_3(CO)_9S$ by an iron atom to give $FeCo_2(CO)_9S$, there is likewise an average decrease of 0.039 (1) Å in the metal–metal bond lengths upon the formal substitution of an iron atom in place of one cobalt atom in $Co_3(CO)_9Se$ to give the corresponding $FeCo_2(CO)_9Se$. Hence, this study provides an important operational test of our hypothesis (which motivated this research) that a formal removal of an unpaired electron from a tricobalt enneacarbonyl chalcogen complex by the substitution of an iron for a cobalt atom produces a shortening and hence strengthening of the metal–metal bonds in accord with the highest occupied MO containing the unpaired electron in $Co_3(CO)_9X$ being strongly antibonding relative to the three metal atoms. The particular nature of this antibonding MO is discussed later in connection with the interpretations of the esr data.

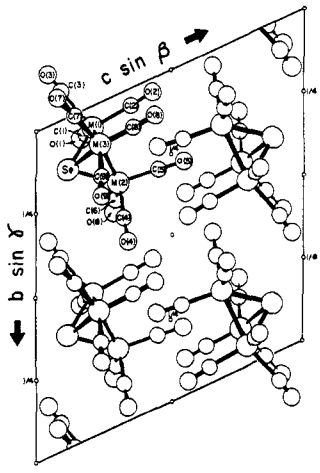

Figure 4. [100] projection of the *C*-centered triclinic unit cell of $Co_3(CO)_9Se$ and of its isomorphous analog $FeCo_2(CO)_9Se$. There is one crystallographically independent molecule in this centrosymmetric cell.

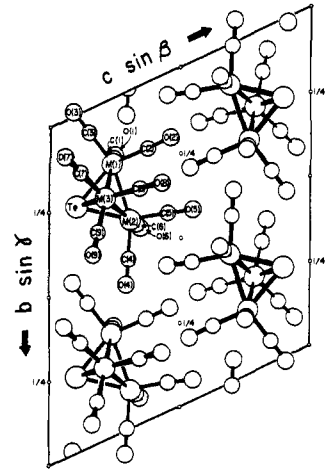

Figure 5. [100] projection of the *C*-centered triclinic unit cell of $FeCo_2(CO)_9Te$. There is one crystallographically independent molecule in this centrosymmetric cell.

A completely unexpected but nevertheless significant aspect of the structural determinations of the $M_3(CO)_9Se$ complexes is that the average metal–metal distance in $Co_3(CO)_9Se$ is *less* by 0.021 (4) Å than that found in $Co_3(CO)_9S$ despite the fact that the formal replacement of the apical sulfur atom with a larger selenium atom would be expected under normal circumstances to cause an *increase* in the Co–Co distances. This observation along with the decreased *antibonding* effect of the unpaired electron on the metal–metal distances in the two selenium structures compared to the corresponding sulfur structures points to the increased influence of the M–Se bonding relative to the M–S bonding on the overall molecular geometry (*i.e.*, while occupation of the antibonding orbital in $Co_3(CO)_9Se$ tends to increase the metal–metal distance, such a change presumably is more constrained by the metal–chalcogen σ-bonding framework in this case than in the case of $Co_3(CO)_9S$). These conclusions emphasize that the influence of the unpaired electron in $Co_3(CO)_9X$ on its molecular geometry is just one of many factors relating to the equilibration of the atoms at given internuclear distances. Hence, although a quantitative estimation of the effect of bonding or antibonding electrons on molecular geometries apparently cannot be predicted, it is illustrated here that in a given organometallic cluster system it is definitely possible from the resulting directional shifts of the metal atoms upon alteration of the number of valence electrons by formal substitution of a different metal atom to deduce the topological nature of the highest occupied metal symmetry orbital.

Another important stereochemical principle exemplified by this series of $M_3(CO)_9X$ complexes is that the difference in metal–metal distances for the three electronically equivalent diamagnetic molecules $FeCo_2(CO)_9X$ (X = S, Se, Te) is less than 0.05 Å, in contradistinction to the relatively large observed increases in the two types of Co–Co distances of 0.28 (2) and 0.10 (2) Å for the octahedrally shaped Co_4X_2 cluster system

found in the diamagnetic series of molecules $Co_4(CO)_{10}X_2$ (X = S, Te) upon substitution of the congener tellurium for sulfur. These dissimilarities in changes of the metal–metal distances upon formal replacement of the bridging sulfur atoms with tellurium atoms in these two different series of metal cluster complexes signify that one must be extremely careful either in an extrapolation of trends in molecular parameters or in the formulation of bonding generalizations from one kind of metal cluster system to another kind of metal cluster system of different basic geometry. As in the case for the sulfur analogs, the difference in the average metal–chalcogen distances of $FeCo_2(CO)_9Se$ and $Co_3(CO)_9Se$ is probably not significant. The differences in the average metal–chalcogen distances in the series $M_3(CO)_9X$ (X = S, Se, Te) are in excellent agreement with those predicted by the change in covalent radii of the chalcogen atoms. The observed average variations in metal–chalcogen bond lengths between the $Co_3(CO)_9S$–$Co_3(CO)_9Se$ and $FeCo_2(CO)_9S$–$FeCo_2(CO)_9Se$ pairs are 0.14 and 0.13 Å, respectively, *vs.* a difference of 0.13 Å between the estimated covalent radii of sulfur (1.04 Å)[24] and selenium (1.17 Å),[24] while the observed average variation in the metal–chalcogen distance between the $FeCo_2(CO)_9Se$–$FeCo_2(CO)_9Te$ pair is 0.18 Å *vs.* a difference of 0.20 Å based on the estimated covalent radii of selenium and tellurium (1.37 Å).[24]

No significant differences are found in either the metal–carbon or the carbon–oxygen distances for the three structural determinations.

Stereochemical Interrelationships Based on the Esr Data. From a detailed analysis of the combined information obtained from the esr solution spectrum and the anisotropic esr single-crystal spectrum, the unpaired electron in $Co_3(CO)_9S$ was unambiguously assigned to the nondegenerate MO of antibonding metal character shown in Figure 6. This orbital of a_2 representation is constituted primarily of the in-plane cobalt $3d_{xz}$ orbitals (labeled on the basis of an arbitrarily defined local orthogonal right-handed coordinate system on each cobalt atom, wherein the positive z axis is directed toward the centroid of the three cobalt atoms and the x axis is in the plane of the three cobalt atoms). The fact that such an a_2 orbital can possess no cobalt s character is completely consistent with the observation that the hyperfine coupling constant of 30.9 G for $Co_3(CO)_9S$ is just one-third that of several other cobalt compounds in which the unpaired electron is localized in a single cobalt d orbital.[5] Spin polarization of the inner s electron by an electron occupying an a_2 orbital was shown by McGarvey[25] to give rise to a negative cobalt isotropic hyperfine coupling constant. From the magnitude of the hyperfine coupling constant ($A_{||}$) observed when the threefold axis of the $Co_3(CO)_9S$ molecule is parallel to the magnetic field direction, it was deduced[5] that the isotropic and dipolar contributions to $A_{||}$ must have the same sign, and furthermore that the principal symmetry axes of the cobalt atomic d orbitals comprising the half-filled molecular orbital must be nearly parallel to the molecular threefold axis. Based on this model the magnitude of the hyperfine term $|A_{||}|$ was calculated

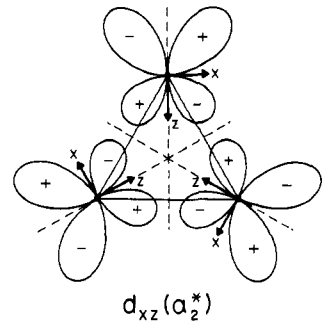

Figure 6. The nondegenerate antibonding metal symmetry orbital combination (of a_2 representation) comprised of d_{xz} orbitals localized in the plane of metal atoms. A detailed analysis of the esr data provided definitive evidence that the one unpaired electron in $Co_3(CO)_9S$ and in $Co_3(CO)_9Se$ resides in this antibonding tricobalt orbital which has nodal planes coincident with the three vertical mirror planes possessed by each of these two isostructural molecules of C_{3v} symmetry.

to be 77.0 G, in excellent agreement with the observed coupling constant of $|A_{||}| = 74.3$ G.[5]

The fact that this strongly antibonding a_2 orbital is orthogonal to all s, p, and d atomic orbitals on the sulfur atom led to the prediction that substitution of a selenium atom for the sulfur atom would cause little change in the hyperfine parameters. The esr study of $Co_3(CO)_9Se$ in solution and in single crystals of $FeCo_2(CO)_9Se$, reported here, confirms this prediction. While the isotropic hyperfine coupling constant of $Co_3(CO)_9Se$ cannot be accurately measured from the solution spectrum, it must be within 5% of that obtained for $Co_3(CO)_9S$. The hyperfine coupling constant $A_{||}$ observed with the magnetic field direction parallel to the idealized threefold axis of the $Co_3(CO)_9Se$ molecule is only 2% less than that observed for $Co_3(CO)_9S$ (72.8 G *vs.* 74.3 G).

Bonding Description and Resulting Stereochemical Implications. The molecular orbital arguments (previously briefly outlined[5]) utilized to rationalize the esr and X-ray diffraction results for $Co_3(CO)_9S$ are not only equally valid for $Co_3(CO)_9Se$ but also sufficiently general that they have been successfully employed to predict observable metal–metal bond length changes in a number of other triangular metal cluster complexes.[26–30] Hence, the application of this qualitative LCAO-MO model to the $Co_3(CO)_9X$ complex is reported here in detail in order to elucidate further the nature of metal–metal interactions in organometallic cluster systems. A local right-handed Cartesian coordinate system is defined at each cobalt atom with the positive z axis directed toward the center of the cobalt triangle, the y axis located perpendicular to the tricobalt plane, and the x axis situated in the tricobalt plane. For this choice of axes, nine sets of three symmetry orbitals of a given type can be constructed under C_{3v} molecular symmetry from the nine types of valence orbitals per cobalt atom. Since the three 4s and nine 4p tricobalt orbital combinations of representations

(24) *Cf.* F. A. Cotton and G. Wilkinson, "Advanced Inorganic Chemistry," 2nd ed, Interscience, New York, N. Y., 1966, p 105.
(25) B. R. McGarvey, *J. Phys. Chem.*, 71, 51 (1967).
(26) H. Vahrenkamp, V. A. Uchtman, and L. F. Dahl, *J. Amer. Chem. Soc.*, 90, 3272 (1968).
(27) H. Vahrenkamp and L. F. Dahl, *Angew. Chem., Int. Ed. Engl.*, 8, 144 (1969).
(28) V. A. Uchtman and L. F. Dahl, *J. Amer. Chem. Soc.*, 91, 3763 (1969).
(29) V. A. Uchtman and L. F. Dahl, submitted for publication.
(30) P. D. Frisch and L. F. Dahl, to be published.

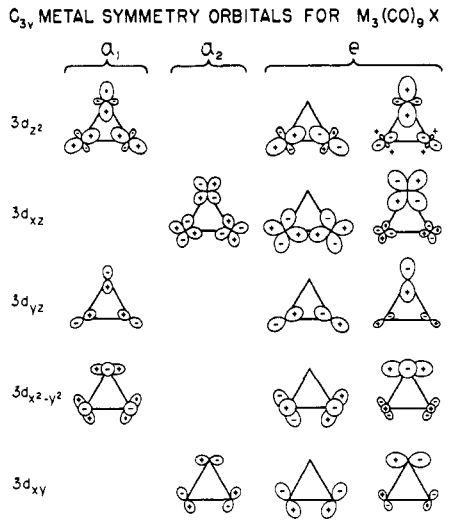

Figure 7. Classification under C_{3v} symmetry of the five sets of 3d metal symmetry orbitals available for metal–metal interactions in the $M_3(CO)_9X$ molecule.

$3a_1 + a_2 + 4e$ possess the proper symmetry and directional properties for effective σ bonding of the cobalt atoms to the sulfur and carbonyl ligands, it is arbitrarily assumed that only these 4s and 4p cobalt basis functions are utilized to form localized cobalt–ligand σ bonds. The presumption of the perfect-pairing approximation then allows separability of the metal–ligand σ-bonding interactions from the metal–metal interactions. Although these simplifying assumptions are not valid from the viewpoint of a rigorous quantitative description of the electronic structure, nevertheless the bonding picture obtained from this particular MO model appears to be correct qualitatively with regard to existing data and resulting stereochemical predictions which have been operationally tested.[1,5,26-30]

The remaining five sets of 3d cobalt symmetry orbital combinations (of total representations $3a_1 + 2a_2 + 5e$) which are available for direct cobalt–cobalt interactions are shown in Figure 7. If it is further assumed that the energy level splittings from the cobalt–cobalt interactions are sufficiently large compared to the splittings due to nonspherical field effects, then orbital overlap considerations predict (with the neglect of any configurational interaction) that the lowest two energy levels will be the in-plane tricobalt bonding $d_{z^2}(a_1)$ and $d_{xz}(e)$ orbitals while the highest two energy levels will be the corresponding in-plane tricobalt antibonding $d_{xz}(a_2^*)$ and $d_{z^2}(e^*)$ combinations. However, in the qualitative energy level diagram given in Figure 8 the atomic orbital character of the energy levels is not specified, since mixing can occur among the tricobalt symmetry orbitals belonging to the same representation. Invarient to the unknown degree of mixing, it is noteworthy that all three metal symmetry orbitals of a_1 representation will be bonding orbitals, while both those of a_2 representation will be antibonding relative to the energies of the isolated atomic orbitals of each cobalt atom. Furthermore, only the specific orbitals comprising the highest two energy levels, labeled $2a_2$ and 5e in Figure 8, are of particular importance to this discussion.[31]

(31) MO calculations are being carried out (B. K. Teo, M. B. Hall, R. F. Fenske and L. F. Dahl, to be published) on $Co_3(CO)_9S$ and its relatives *via* the LCAO approach with a nonparameterized model (*cf.* M. B. Hall and R. F. Fenske, *Inorg. Chem.*, submitted for publication, and references cited therein for details of the approximations and computational techniques). For $Co_3(CO)_9S$ preliminary MO calculations indicate that the a_2 level containing the unpaired electron is comprised primarily of tricobalt d_{xz} orbitals of antibonding character (in accord with the esr analysis[5]) along with some mixing of tricobalt p_x orbitals. The results of this and several other metal-cluster complexes not only exhibit extensive mixing of the orbitals for an occupied level of given representation but also demonstrate that the relative energy level ordering is strongly dependent on metal–ligand interactions as well as metal–metal interactions. Nevertheless, the simplified bonding model given in this paper conceptually provides a reasonable qualitative basis in the prediction of expected observational changes as well as an accounting of the determined variations in the molecular geometries of metal cluster systems.

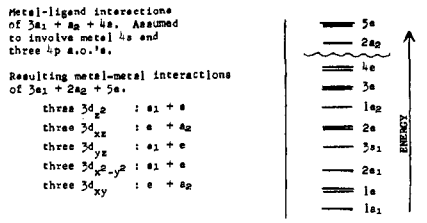

Figure 8. Qualitative energy-level scheme for the metal symmetry orbitals in the C_{3v} $M_3(CO)_9X$ molecule.

In the $Co_3(CO)_9X$ molecule the triply bridging chalcogen atom may be reasonably considered to have a tetrahedral-like valency of one nonbonding and three bonding electron pairs, with the unshared electron pair localized along the molecular threefold axis and with the other four valence electrons of the chalcogen atom participating in σ bonding with the three cobalt atoms. Hence, of the 27 valence electrons made available by the tricobalt system, two of them must be utilized to complete the three electron-pair σ bonds with the chalcogen atom. A distribution of the remaining 25 electrons *via* the *aufbau* principle into the available tricobalt energy levels portrayed in Figure 8 leads to the unpaired electron occupying the nondegenerate $2a_2$ level. The fact that the esr studies of both $Co_3(CO)_9S$ and $Co_3(CO)_9Se$ establish that the unpaired electron must be in this antibonding a_2^* orbital and that this tricobalt orbital is comprised primarily of the in-plane antibonding combination of d_{xz} atomic orbitals is in accord with our qualitative MO model.

A significant bonding principle which therefore emanates from these investigations is the self-consistency between the MO model employed here and the equivalent valence-bond formalism concerning the fact that in a triangular metal-cluster system any electrons in excess of the closed-shell electronic configuration of each metal atom occupy primarily the in-plane antibonding metal σ-orbital combinations. In Figure 8 the "noble gas" electronic configuration for each metal atom in either the $FeCo_2(CO)_9X$ molecules (of assumed C_{3v} geometry) or the oxidized $Co_3(CO)_9X^+$ cation corresponds to the available 24 electrons occupying all levels through the 4e one. The wavy line above this level signifies that for such a noble gas metal complex the highest two levels, $2a_2$ and 5e, are empty. The conversion of such an MO picture with the bonding $d_{z^2}(a_1)$ and $d_{xz}(e)$ combinations filled with six electrons and (with the corresponding antibonding $d_{xz}(a_2^*)$ and $d_{z^2}(e^*)$ ones empty) to a valence-bond counterpart involving electron-pair metal–metal bonds is made apparent once it is recognized that the *net* contribution to the metal–metal interactions in this triangular metal

system merely involves the distribution of the six electrons in the bonding in-plane cobalt symmetry orbitals. From the d_{z^2} and d_{xz} atomic orbitals at each cobalt atom, two equivalent hybrid orbitals $d_{z^2} \pm d_{xz}$ may be constructed which can form localized bonding and antibonding σ-orbital combinations by overlap with the corresponding identical hybrid orbitals on the other two cobalt atoms. An electron-pair bond between each pair of cobalt atoms is therefore a consequence of the placement of six available electrons in the three bonding σ-orbital combinations. It follows that the effect of the extra 25th electron in the $Co_3(CO)_9X$ molecule (by its occupation of the antibonding in-plane tricobalt $2a_2$ symmetry orbital) is to reduce the valence-bond metal–metal order to *less* than one.

We wish to predict that the one unpaired electron in the recently prepared black, paramagnetic complex $Ni_3(h^5\text{-}C_5H_5)_3(tert\text{-}C_4H_9N)$,[32] which is electronically equivalent and structurally analogous[33] to the $Co_3(CO)_9X$ (X = S, Se) molecules, is similarly in an antibonding metal symmetry orbital (rather than in a bonding one as speculated by its synthesizers[32]). An attempt is in progress to obtain an operational test of our hypothesis by comparison of the metal–metal bond lengths in this complex with those of its (as yet unknown) diamagnetic analog. It is hoped that production of such an analog by removal of the unpaired electron from $Ni_3(h_5\text{-}C_5H_5)_3(tert\text{-}C_4H_9N)$ can be achieved either by oxidation of the parent molecule to give the monocation or by substitution of a cobalt atom in place of one nickel atom (such as was successfully done[29] to prove operationally that the unpaired electron in $Ni_3(h^5\text{-}C_5H_5)_3(CO)_2$ was also in an antibonding metal symmetry orbital rather than in a bonding one as previously reported[34]).

Acknowledgments. We are most pleased to thank the National Science Foundation (Grant No. GP-4919X) for financial sponsorship of this work. The use of the UNIVAC 1108 and CDC 3600 computers at the University of Wisconsin Computing Center was made possible by partial support of the National Science Foundation and the Wisconsin Alumni Research Foundation administered through the University Research Committee. One of us, C. E. S., is grateful to the National Science Foundation for a Predoctoral NSF Trainee Fellowship.

(32) S. Otsuka, A. Nakamura, and T. Yoshida, *Justus Liebigs Ann. Chem.*, **719**, 54 (1968); *Inorg. Chem.*, **7**, 261 (1968).

(33) A single-crystal X-ray diffraction study[32] of $Ni_3(h^5\text{-}C_5H_5)_3(tert\text{-}C_4H_9N)$ showed its idealized C_{3v} molecular geometry to be closely related to that of $Co_3(CO)_9X$ (X = S, Se) with the triply bridging NR ligand symmetrically attached to the equilateral triangle of nickel atoms and with each cyclopentadienyl ring occupying the three coordination sites in place of three carbonyl ligands. The experimental conformity of this molecule to a C_{3v} geometry is based on assumed cylindrical symmetry for each cyclopentadienyl ring. The average value for the three Ni–Ni distances is 2.35 Å.

(34) H. C. Longuet-Higgins and A. J. Stone, *Mol. Phys.*, **5**, 417 (1962).